Journal of the American College of Cardiology Vol. 47, No. 5, 2006

Published by Elsevier Inc.
ISSN 0735-1097/06/$32.00
doi:10.1016/j.jacc.2005.08.076

PRECLINICAL STUDY

Adventitial Microvessel Formation After Coronary Stenting and the Effects of SU11218, a Tyrosine Kinase Inhibitor

Asim N. Cheema, MD, PHD, FACC,* Tony Hong,* Nafiseh Nili, PHD,* Amit Segev, MD,* John G. Moffat, PHD,† Kenneth E. Lipson, PHD,† Anthony R. Howlett, PHD,† David W. Holdsworth, PHD,‡ Michael J. Cole, MESC,‡ Beiping Qiang, MD,* Frank Kolodgie, PHD,§ Renu Virmani, MD, FACC,§ Duncan J. Stewart, MD, FACC,* Bradley H. Strauss, MD, PHD, FACC*

Toronto and London, Ontario, Canada; South San Francisco, California; and Washington, DC

OBJECTIVES The aim of this study was to delineate the temporal profile of adventitial microvessel (Ad-MV) formation after stenting, its relationship to arterial wall hypoxia, and the effects of a tyrosine kinase inhibitor (TKI), SU11218, on Ad-MV and in-stent intimal hyperplasia (IH).

BACKGROUND Adventitial microvessels have been reported after arterial injury; however, the underlying stimulus for this response and its relationship to IH is unknown.

METHODS Coronary stenting was performed in 40 pigs randomized to SU11218 (n = 20) or placebo (n = 20). Vessel wall hypoxia was assessed by pimonidazole adducts and hypoxia-inducible factor (HIF)-1 alpha expression. Adventitial microvessels were quantified by three-dimensional microscopic computed tomography (3D micro CT). Intimal hyperplasia was measured by intravascular ultrasound (IVUS), 3D micro CT, and morphometry. The effects of SU11218 were assessed in vitro on smooth muscle cell (SMC) and endothelial cell (EC) functions and in vivo on Ad-MV and IH.

RESULTS Hypoxia was evident in the vessel wall at 48 h and persisted for four weeks. Adventitial microvessels increased significantly at one week (24 ± 7 microvessels/segment) and four weeks (23 ± 7 microvessels/segment) compared with uninjured arteries (16 ± 2 microvessels/segment; $p < 0.001$) and correlated with IH ($r = 0.77$, $p < 0.001$). The TKI SU11218 inhibited platelet-derived growth factor receptor–beta phosphorylation, EC and SMC DNA synthesis, and migration in a dose-dependent manner in vitro and significantly inhibited Ad-MV (16 ± 5 vs. 23 ± 7 microvessels/segment in placebo, $p < 0.001$) and produced approximately 80% reduction in IH (0.52 ± 0.51 mm^2 vs. 2.47 ± 1.66 mm^2 in placebo, $p < 0.001$) at four weeks in vivo.

CONCLUSIONS Arterial stenting causes arterial wall hypoxia followed by Ad-MV formation. The TKI SU11218 inhibits both Ad-MV formation and IH and represents a promising therapeutic agent to prevent in-stent restenosis. (J Am Coll Cardiol 2006;47:1067–75) © 2006 by the American College of Cardiology Foundation

The precise role of the adventitial layer in modulating the neointimal response after coronary stenting remains unclear. Previous studies have indicated that adventitial myofibroblasts might migrate toward the arterial lumen and contribute to intimal hyperplasia (1). Other studies have described changes in the extracellular matrix within the adventitia (2,3). Recently, there has been growing interest in the potential role of the adventitial vasa vasorum in the arterial repair process after injury. Although an increase in adventitial microvessels (Ad-MV) has been reported after experimental balloon injury (4,5), the underlying stimuli leading to the Ad-MV response have not been elucidated and it is unknown whether a similar response is present after arterial stenting.

Tissue hypoxia is a potent stimulus for expression of vascular endothelial growth factor (VEGF) and platelet-derived growth factor (PDGF) (6,7), two growth factors that play critical roles in the formation of new blood vessels. The VEGF initiates angiogenesis by stimulating endothelial cell (EC) proliferation and the formation of endothelial tubes, whereas PDGF and its receptor, platelet-derived growth factor receptor-beta (PDGFR-β), play a central role in the recruitment of pericytes and smooth muscle cell (SMC) to form stable and mature microvessels (8,9). Both VEGF and PDGF receptors mediate cell signaling through receptor tyrosine kinases that might serve as an important target for the development of novel anti-angiogenic therapies (10,11).

From the *Roy and Ann Foss Cardiovascular Research Program, Terrence Donnelly Heart Center, St. Michael's Hospital, University of Toronto, Toronto, Ontario, Canada; †SUGEN, Inc., South San Francisco, California; ‡Robarts Research Institute, London, Ontario, Canada; and the §Department of Cardiovascular Pathology, Armed Forces Institute of Pathology, Washington, DC. Supported by the Canadian Institute of Health Research (grant no. MOP-53325) and dedicated to the memory of Robyn Strauss Albert. Dr. Segev was a Research Fellow of the Heart and Stroke Foundation of Canada. Drs. Moffat, Lipson, and Howlett were employees of SUGEN, Inc., South San Francisco, California, at the time the study was conducted. Dr. Holdsworth is a Career Investigator of the Heart and Stroke Foundation of Ontario.

Manuscript received June 10, 2005; revised manuscript received August 11, 2005, accepted August 15, 2005.

JACC Vol. 47, No. 5, 2006
March 7, 2006:1067–75

Abbreviations and Acronyms

3D micro CT	= three-dimensional microscopic computed tomography
Ad-MV	= adventitial microvessels
BrdU	= bromo-dexoyuridine
CA-EC	= coronary artery endothelial cells
CA-SMC	= coronary artery smooth muscle cells
CSA	= cross-sectional area
EC	= endothelial cells
HIF	= hypoxia-inducible factor
IH	= in-stent intimal hyperplasia
IVUS	= intravascular ultrasound
PDGF	= platelet-derived growth factor
SMC	= smooth muscle cells
TKI	= tyrosine kinase inhibitor
VEGF	= vascular endothelial growth factor

In this study we assessed serial changes in Ad-MV in a porcine coronary stenting model and the presence of tissue hypoxia as a stimulus of such changes. Furthermore, we administrated SU11218, a class III tyrosine kinase inhibitor (TKI), to study the effects of VEGF and PDGF receptor inhibition on Ad-MV formation and intimal hyperplasia (IH).

METHODS

Animal model. Experiments were performed in accordance with guidelines set out by the University of Toronto and approved by the St. Michael's Hospital Animal Care Committee. Coronary stenting was performed in 40 castrated male Yorkshire pigs weighing 25 to 30 kg as summarized in Figure 1. Animals received intravenous heparin (200 U/kg), and stents (EXPRESS, Boston Scientific, Inc., Natick, Massachusetts) were deployed in the circumflex artery, with a 1:1 stent-to-artery ratio. Intravascular ultrasound (IVUS) was performed with a 40-MHz UltraCross (Boston Scientific, Inc.) catheter before and after the procedure. All animals received aspirin 325 mg daily. Repeat angiography was performed at end study (48 h, 1 week, or 4 weeks). Intravascular ultrasound follow-up was only done at four weeks. Animals were treated with either subcutaneous injections of placebo or the TKI SU11218 (5 mg/kg, SUGEN, Inc., San Francisco, California), twice a week for 4 weeks, starting 1 day before stenting. This dosing schedule achieved a mean plasma concentration of 3.2 nmol/l (range 2.5 to 5.0 nmol/l, n = 4 pigs) without any adverse effects on histopathology of internal organs (liver, kidney, pancreas, adrenals, skeletal muscle, salivary gland, bone marrow, and myocardial tissue). The molecular weight of SU11218 is 457 Da.

Intravascular ultrasound. Intravascular ultrasound images were analyzed with a digital video analyzer during manual pullback and at regular intervals by an observer blinded to the treatment allocation. Intimal cross-sectional area (CSA) was measured at three sites (proximal, middle, and distal) within the stented segments, and a mean intimal CSA was determined.

Three-dimensional microscopic computed tomography. The arteries were processed and scanned with minor modifications of previously published protocol (4). After sacrifice, hearts were perfused with 500 ml of heparinized saline, followed by 60 to 80 ml of a low-viscosity radio opaque polymer, MV 122 (Flowtech, Inc., Carver, Massachusetts) at 90 mm Hg until it was flowing freely through the coronary sinus. Hearts were placed in 10% buffered formalin at 4° C for 24 h to allow polymerization of the compound. The stented segments were removed and placed in glycerol (30%, 50%, 70%, and 100% for 24 h each) before paraffin embedding. The specimens were scanned with three-dimensional microscopic computed tomography (3D micro CT) (eXplore MS Micro CT, GE Healthcare, London, Canada) at 90 kVp (75 μA) with a filter composed of copper (0.25 mm) and aluminum (0.25 mm) to reduce CT artifacts from stent struts. Images were acquired at 0.5°-steps over 360° and reconstructed into three-dimensional volumes of 16-μm resolution using true Feldkamp cone beam filtered back projection algorithm (12).

Ad-MV. The 3D micro CT scan of each stented segment was divided into 10 cross-sections, and the number of microvessels in the arterial adventitia (defined as a 1.0-mm annular perimeter around the stent struts) were counted in each cross-section and a segment mean determined (Fig. 2A). Maximum intensity projections were obtained through 3D volume images to assess the spatial distribution of the microvessels (Fig. 2B). In addition, CSA of Ad-MVs was measured with computerized image analysis software (Image J, Bethesda, Maryland) in five cross-sections of each stented artery and a mean Ad-MV CSA was determined in a 4-week group of placebo- and SU11218-treated animals.

Morphometric measurements. After scanning, stented segments were embedded in plastic and cut into 4-μm-thick

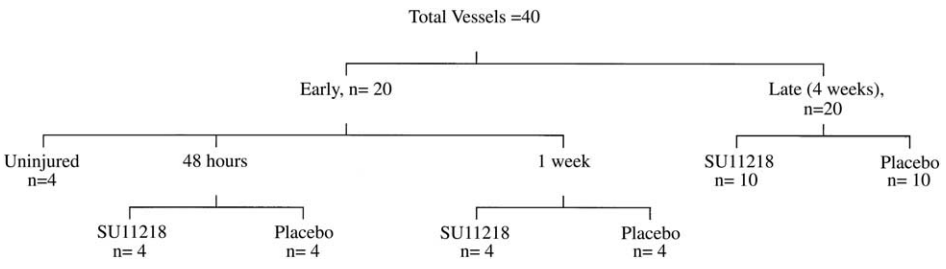

Figure 1. Study protocol: the number of vessels analyzed and time points studied.

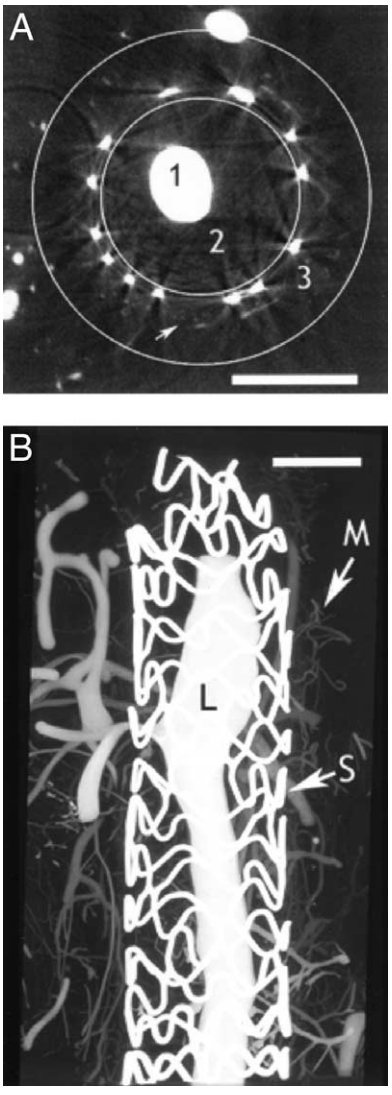

Figure 2. Cross-sectional **(A)** and maximum intensity projection **(B)** images of a three-dimensional microscopic computed tomography (3D micro CT) scan of stented artery for assessment of adventitial microvessels (Ad-MV). **(A)**, radio-opaque contrast can be seen in the main artery as well in the Ad-MV **(arrow)**. Contrast-filled microvessels were counted in the media/adventitia, defined as a 1.0-mm annular area surrounding the stent struts. **1** = lumen cross-sectional area (CSA); **2** = intima CSA; **3** = arterial media/adventitia. **(B)**, 3D micro CT shows detail of Ad-MV around stent struts. **White bars** = 2 mm.

sections. Movat pentachrome stained sections obtained from three sites (proximal, mid, and distal) within the stented segment were used to assess injury scores according to Schwartz et al. (13). Lumen and intimal CSA were measured with image analysis software (Scion, Frederick, Maryland).

Tissue hypoxia. Animals were injected with 200 mg of pimonidazole (Hypoxyprobe, Chemicon International, Inc., Temecula, California) intravenously 60 min before tissue harvesting. Pimonidazole forms irreversible adducts with intracellular macromolecules under hypoxic conditions (14). This technique identifies tissue pO_2 levels of <10 mm Hg (15). For western immunoblotting, tissue extracts containing 50 μg of proteins were separated by 4% to 20% sodium dodecyl sulphate polyacrylamide gels (SDS-PAGE) and electrotransferred onto a nitrocellulose membrane. Membranes were immunoblotted with anti-pimonidazole monoclonal antibody (Chemicon International, Inc.) for detection of pimonidazole adducts. Western immunblotting was also performed under the same conditions with anti–hypoxia-inducible factor (HIF)-1alpha monoclonal IgG 2b (Clone H1alpha67, Novous Biologicals, Littleton, Colorado) for HIF-1 alpha expression. Detection was performed with a chemiluminescence peroxidase detection system (Sigma, St. Louis, Missouri) and exposure to BioMax film (Kodak, Rochester, New York). Ischemic skeletal muscle from porcine lower hind limb, obtained 6 h after occlusion of external iliac artery, served as a positive control. Protein loading was assessed by Ponceau-red staining. Densitometric analysis of the immuno bands for HIF-1 alpha, pimonidazole adducts, and the ponceau red bands was performed with ImageQuant TL software (Amersham Biosciences Corp., Piscataway, New Jersey) to correct for protein loading. Immunohistochemistry was done on arterial cross-sections with the anti-piminidazole antibody (1: 200 dilution).

SU11218 in vitro studies. Human CA-SMC and CA-EC were obtained from Clonetics (Cambrex, Inc., East Rutherford, New Jersey) and maintained in SmGM-2 and EGM-2MV medium, respectively.

DNA synthesis. The effects of SU11218 on CA-SMC and CA-EC DNA synthesis were assessed by bromodexoyuridine (BrdU) incorporation. Quiescent cells were exposed to increasing concentrations of SU11218 and stimulated with either PDGF (100 ng/ml, Roche Molecular, Indianapolis, Indiana) or VEGF (20 ng/ml, R & D Systems, Minneapolis, Minnesota) for CA-SMC and CA-EC, respectively. After 16 h, BrdU was added to the cultures for two additional hours of incubation. The cells were then fixed and BrdU incorporation was assessed by ELISA (Roche Diagnostics).

Migration assay. Cells were made quiescent by overnight incubation in basal medium (Cambrex Corp., East Rutherford, New Jersey) supplemented with 0.5% fetal bovine serum. Cells were then labeled with 10 μmol/l Calcein AM (Molecular Probes, Inc., Eugene, Oregon) for 1 h, trypsinized, washed, counted, and placed in basal medium supplemented with 0.5% fetal bovine serum, insulin, transferring, and selenium (Invitrogen, Carlsbad, California) in 24-well FluoroBlok membrane inserts with an 8-μm pore size (BD Biosciences, Bedford, Massachusetts). The TKI SU11218 was added to both the upper and lower chambers in duplicate wells at the indicated concentrations for 10 min, followed by PDGF-BB (CA-SMC) or VEGF (CA-EC) addition to the lower chambers. Four hours later the fluorescence microscope images of the lower surface of the inserts were recorded, and the number of migrated cells was quantified with ImagePro software (MediaCybernetics, San Diego, California). Two low-power fields were captured and quantified for

JACC Vol. 47, No. 5, 2006
March 7, 2006:1067–75

each well. The results were expressed as number of migrated cells as a percent of total cells.

PDGFR-β phosphorylation. The CA-SMC were starved for 48 h in basal medium containing 0.2% fetal bovine serum before stimulation with 50 ng/ml of PDGF-BB for 5 min. The cells were lysed with HNTG/VO_4 and receptors immunoprecipitated with anti-PDGFR-β polyclonal antibodies (No. 06-498, Upstate Biotechnology, Lake Placid, New York). After fractionation by SDS-PAGE, blots were probed for tyrosine phosphorylation with PY99-biotin (Santa Cruz Biotechnology, Santa Cruz, California) and for protein loading with anti-PDGFR-β (Santa Cruz Biotechnology).

Statistical analysis. All measurements were expressed as mean ± SD. Analysis of variance was performed to compare Ad-MV number and intimal CSA by 3D micro CT, in SU11218-treated versus untreated, stented arteries at each time point. A Bonferroni correction was applied to adjust for multiple comparisons. Student's *t* test was used to compare Ad-MV CSA by 3D micro CT, injury scores and intima thickness by morphometry, and intimal CSA by IVUS between SU11218 and the placebo-treated animals at the four-week time point. For the migration assays, Dunnett's *t* test was used to compare the mean of each SU11218-treated group with the mean positive control (PDGF-stimulated CA-SMC and VEGF-stimulated CA-EC). Pearson's correlation coefficient was performed to assess the relationship between the number of Ad-MV and in-stent intimal CSA. Statistical significance was defined as $p < 0.05$.

RESULTS

Effects of stenting on Ad-MV. Arterial stenting resulted in a significant increase in the number of Ad-MV/segment at 1 week (24 ± 7 vs. 16 ± 2 in uninjured, $p = 0.02$) that persisted up to 4 weeks (23 ± 7 vs. 16 ± 2 in uninjured, $p = 0.02$) (Fig. 3A).

Relationship between Ad-MV and IH. At 4 weeks after stenting, the number of Ad-MV was highly correlated ($r = 0.77$, $p < 0.001$) with in-stent intimal CSA (Fig. 3B). Although Ad-MV and IH both increased after stenting, the ratio of Ad-MV to intimal CSA was significantly higher at 1 week compared with 4 weeks after stenting (26.72 ± 3.17 vs. 8.37 ± 6.05, respectively, $p < 0.001$) (Fig. 3C).

Tissue hypoxia after stenting. The HIF-1 alpha expression was increased in the arterial wall at 1 week and at 4 weeks compared with uninjured arteries (Fig. 4A). Vessel wall hypoxia, based on pimonidazole adducts, was evident at 48 h, 1 week, and 4 weeks after stenting compared with> uninjured arteries (Fig. 4B). Immunohistochemistry (Fig. 4C) localized the tissue hypoxia to the medial/adventitial border of the arterial wall. No tissue hypoxia was present in uninjured arteries treated with pimonidazole (Fig. 4B).

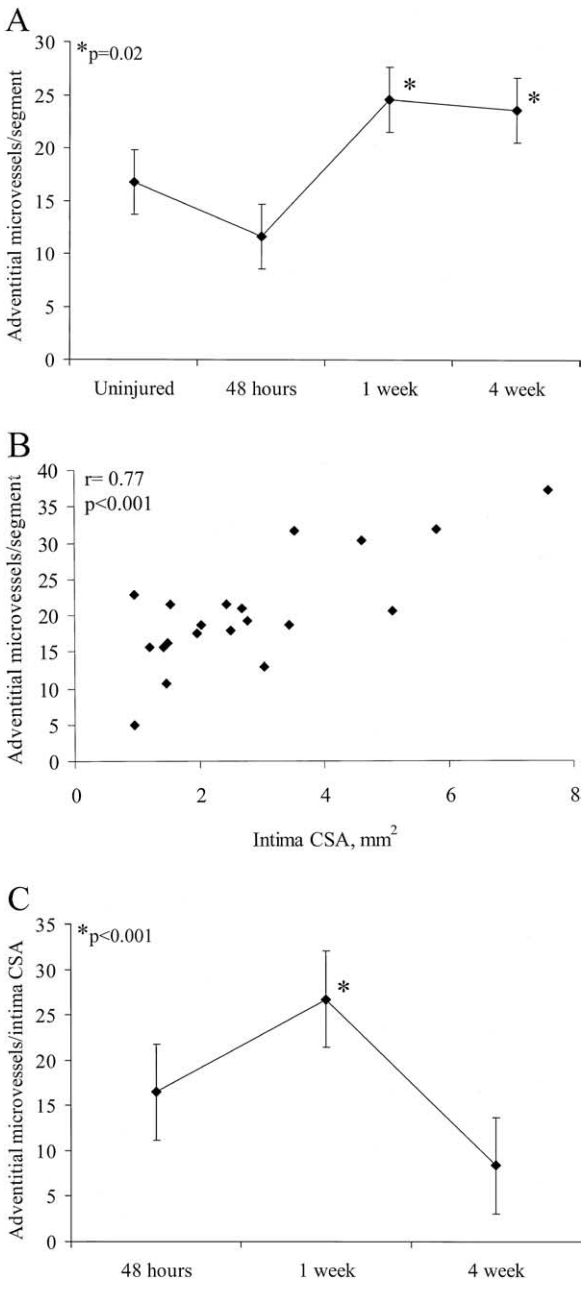

Figure 3. Temporal profile of Ad-MV after stenting. **(A)** A marked increase in the number of microvessels was present at both 1 week and 4 weeks. **(B)** Correlation between Ad-MV and in-stent intimal hyperplasia (IH) at 4 weeks. **(C)** Number of Ad-MV to intimal cross-sectional area (CSA) ratio was significantly higher at 1 week compared with 4 weeks after stenting.

Effects of SU11218 in vitro. DNA SYNTHESIS. The TKI SU11218 inhibited PDGF-stimulated CA-SMC proliferation in a dose-dependent manner, with an IC_{50} value of 25 nmol/l (Fig. 5A). The compound also inhibited VEGF-induced CA-EC proliferation in a dose-dependent manner, with an IC_{50} value of 67 nmol/l (Fig. 5B).

CELL MIGRATION. The TKI SU11218 resulted in a significant inhibition of both PDGF-induced CA-SMC migration and VEGF-induced CA-EC migration at 0.1 μmol/l concentration (Figs. 5C and 5D).

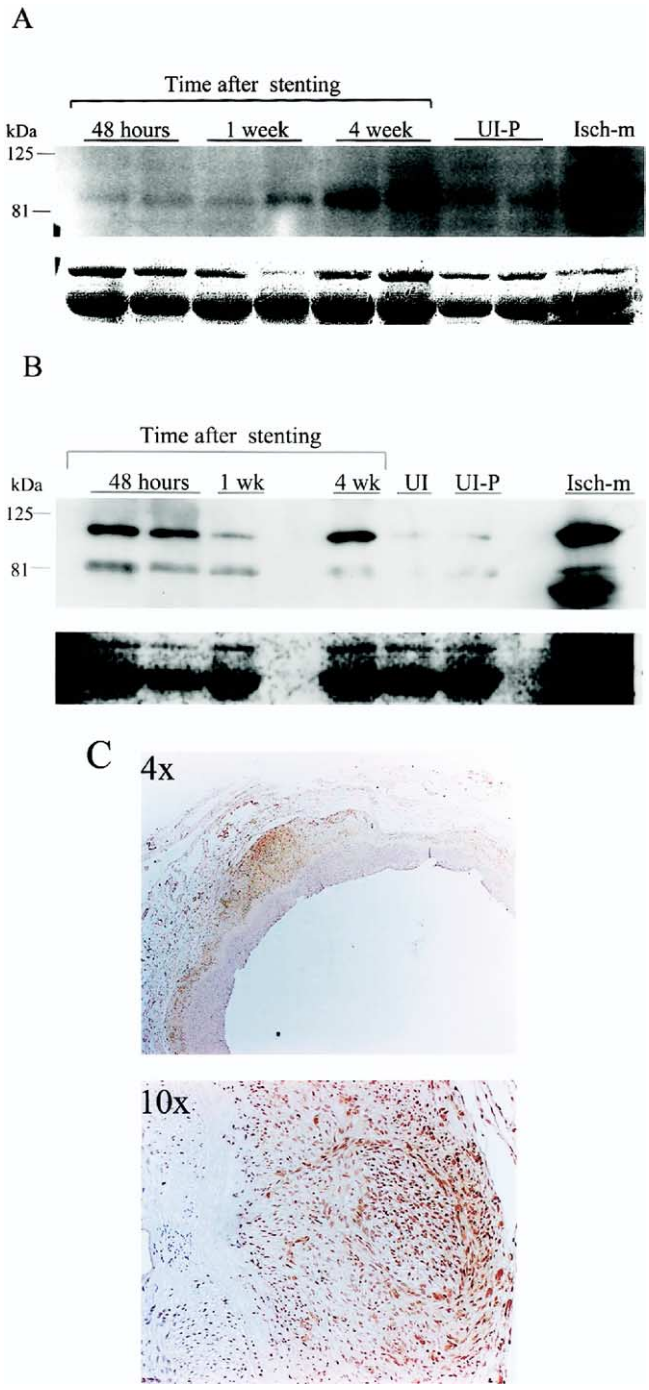

Figure 4. Tissue hypoxia in the arterial wall. **(A)** Hypoxia-inducible factor (HIF)-1 alpha expression was increased at all time points after stenting **(upper panel)**. **(B)** Pimonidazole adducts were identified at all time points after stenting **(upper panel)**. Protein loading was assessed by Ponceau-red staining **(lower panel of A and B)**. **(C)** Immunohistochemistry showing pimonidazole adducts **(stained brown)** at the media/adventitia border at 1 week after stenting. Isch-m = ischemic muscle + pimonidazole; UI = uninjured artery; UI-P = uninjured + pimonidazole.

PDGFR-B PHOSPHORYLATION. The TKI SU11218 resulted in nearly complete inhibition of PDGF-induced phosphorylation of PDGFR-β at 0.1 μmol/l (Fig. 6). These differences in receptor phosphorylation were not due to an altered numbers of receptors, as demonstrated by a parallel blot of PDGFR-β protein.

Effects of SU11218 in vivo. AD-MV. The TKI SU11218 significantly inhibited the formation of Ad-MV at 1 week (9 ± 2 Ad-MV/segment vs. 24 ± 7 in placebo-treated animals, $p < 0.001$) and 4 weeks (16 ± 5 Ad-MV/segment vs. 23 ± 7 in placebo-treated animals, $p < 0.001$) after stenting (Figs. 7A and 8). In addition, the mean Ad-MV CSA was significantly reduced in SU11218-treated animals (0.15 ± 0.05 mm^2 vs. 0.25 ± 0.04 mm^2 in the placebo-treated animals, $p < 0.008$) at 4 weeks.

IH. The IH was significantly reduced at 4 weeks in the SU11218-treated group compared with placebo by all parameters (IVUS, 3D micro CT, and morphometry). Intravascular ultrasound assessment showed that intimal CSA was reduced by approximately 80% in the SU11218-treated group (0.52 ± 0.51 vs. 2.47 ± 1.66 mm^2 in placebo-treated, $p < 0.001$) (Fig. 7B). The intimal CSA by IVUS and 3D micro CT showed excellent correlation ($r = 0.96$, $p < 0.001$). Morphometric analysis also showed approximately 50% reduction in intimal thickness in SU11218-treated animals (0.13 ± 0.07 mm vs. 0.24 ± 0.13 mm in placebo, $p = 0.03$). There were no differences in injury scores between the two groups.

DISCUSSION

Our results indicate that coronary arterial stenting causes tissue hypoxia in the vessel wall that persists for at least 4 weeks. There is concurrent increased expression of the hypoxia responsive transcription factor, HIF-1 alpha, a potent regulator of the pro-angiogenic growth factors. After an initial decrease in the number of Ad-MVs immediately after stenting, there is a marked increase in Ad-MV. This Ad-MV response precedes the development of IH, and the magnitude of this response significantly correlates with the amount of IH. Furthermore, SU11218, a TKI, significantly inhibits both Ad-MV formation and IH.

An increase in Ad-MV has been shown in several diseases affecting the arterial wall (16–19), but limited information is available regarding their relationship to arterial repair after vascular injury. In balloon-injured coronary arteries, Ad-MV density was increased by 4 weeks after vessel injury and the number of Ad-MV correlated with percent lumen stenosis (4). Pels et al. (5) showed that Ad-MV, evaluated by histology only, occurred within three days after balloon injury. Regression of Ad-MV in this balloon-injury model at the time of arterial narrowing suggested that changes in the adventitial microvasculature might be an important component of arterial remodeling after balloon angioplasty. To date, no study has assessed changes in Ad-MV after coronary stenting.

This study is the first to perform 3D micro CT to quantify Ad-MVs in intact specimens containing metal stents. Although this technique has been previously reported in animal vascular injury models (4,19), its use in

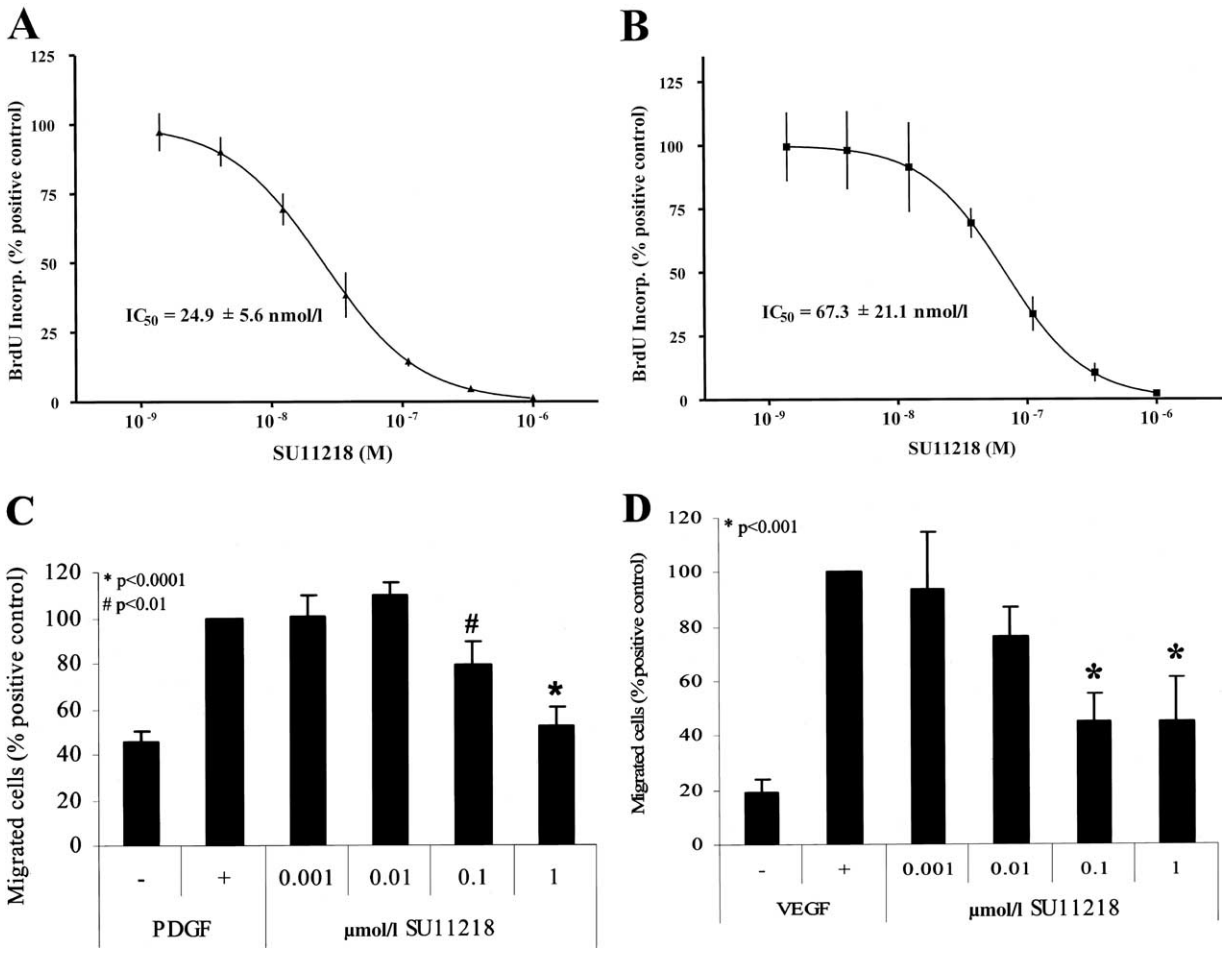

Figure 5. In vitro effects of SU11218. A tyrosine kinase inhibitor, SU11218 inhibited platelet-derived growth factor (PDGF)-stimulated coronary artery smooth muscle cell (CA-SMC) proliferation **(A)**, vascular endothelial growth factor (VEGF)-stimulated coronary artery endothelial cell (CA-EC) proliferation **(B)**, PDGF-stimulated CA-SMC migration **(C)**, and VEGF-stimulated CA-EC migration **(D)** in a dose-dependent manner. BrdU = bromo-dexoyuridine.

coronary stents has been limited by image artifacts associated with the dense metal structure. These artifacts were reduced in this study through the use of a high-quality scan protocol, which included the use of added filtration (copper and aluminum) to reduce beam-hardening artifacts and improve image quality directly adjacent to the stent. The number of Ad-MV in uninjured porcine coronary arteries determined by 3D micro CT was similar to a previous report that used histology (5). In injured vessels, 3D micro CT can accurately identify functioning Ad-MV (with a resolution of 16 μm). In contrast, histology only shows endothelial-lined channels, which might not be functional.

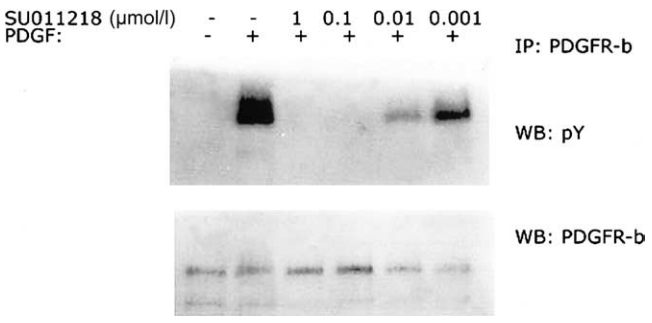

Figure 6. Effects of SU11218 on platelet-derived growth factor receptor-beta (PDGFR-β) phosphorylation. The SU11218 inhibited phosphorylation of the PDGFR-β in a dose dependent manner. The **lower panel** shows equal protein loading of PDFGR-β. IP = immunoprecipitation; pY = phosphorylated PDGFR-beta; WB = Western blot.

Our study demonstrates vessel wall hypoxia is present early after vascular stenting and might be an important stimulus for the angiogenic response. The initial hypoxic response in the medial-adventitial layers after stenting is likely related to the deep vascular injury to the vasa vasorum as a direct consequence of stent deployment, because there was a significant decrease in the number of Ad-MVs at 48 h after stenting. Tissue hypoxia is a potent stimulus for angiogenesis (20,21) and the release of growth factors, such as VEGF (22), PDGF (6,23), endothelin (24), IL-6 (25), and plasminogen activator inhibitor-1 (26), that play a critical role in both neovascularization and the development of intimal hyperplasia. Despite the significant increase in Ad-MV at 1 week and 4 weeks after stenting, arterial wall hypoxia persisted throughout the study period. The progressive thickening of the vessel wall is an important

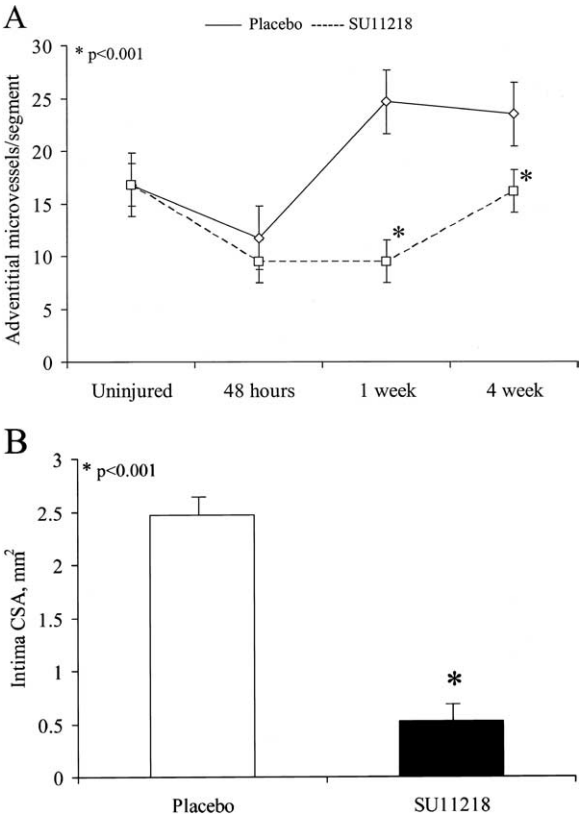

Figure 7. In vivo effects of SU11218. **(A)** The SU11218 significantly inhibited the Ad-MV response after stenting at 1 week and 4 weeks. **(B)** The SU11218 resulted in approximately 80% reduction in the amount of IH at 4 weeks. Abbreviations as in Figures 2 and 3.

determinant of oxygen demand (27) and is likely an important contributor to this ongoing hypoxic response in the vessel wall.

Adventitial microvessel formation is mediated through complex interactions between several growth factors and cytokines. Both VEGF and PDGF are important angiogenic growth factors that mediate cell signaling through receptor tyrosine kinase and are up-regulated during tissue hypoxia (6,22). Whereas VEGF initiates angiogenesis by stimulating EC, PDGF plays a central role in recruitment of pericytes and SMC to form more stable microvessels (8,9). Anti-angiogenic therapies have traditionally targeted VEGF signaling alone, but recent data suggest that blocking PDGFR-β might provide incremental effects (11). We used SU11218 to inhibit angiogenesis in our model, because it targets receptor tyrosine kinases and inhibits both VEGFR and PDGFR-β activation. The TKI SU11218 inhibited in vitro EC and SMC migration and proliferation in a dose-dependent manner. Moreover, SU11218 significantly inhibited both the in vivo adventitial angiogenic response and the formation of IH; however, our study results can not determine the extent to which the effects on IH are related to the inhibition of the Ad-MV or the inhibition of PDGFR-β signaling on intimal SMC.

Angiogenic inhibitors have been successfully used to inhibit the angiogenic response in atherosclerotic lesions and prevent progression of atherosclerosis in apolipoprotein-E–deficient mice (28,29). Inhibition of plaque neovascularization reduced macrophage accumulation and progression of advanced atherosclerosis (29). With regard to vascular injury, there have been conflicting reports on the predominant effect of angiogenic growth factors and inhibitors on arterial repair process (30–37). Although Ad-MV has been previously correlated with neointima formation after non-stent experimental arterial injury (4,34,36), the effects of VEGF expression or blockade on the development of intimal hyperplasia have been variable

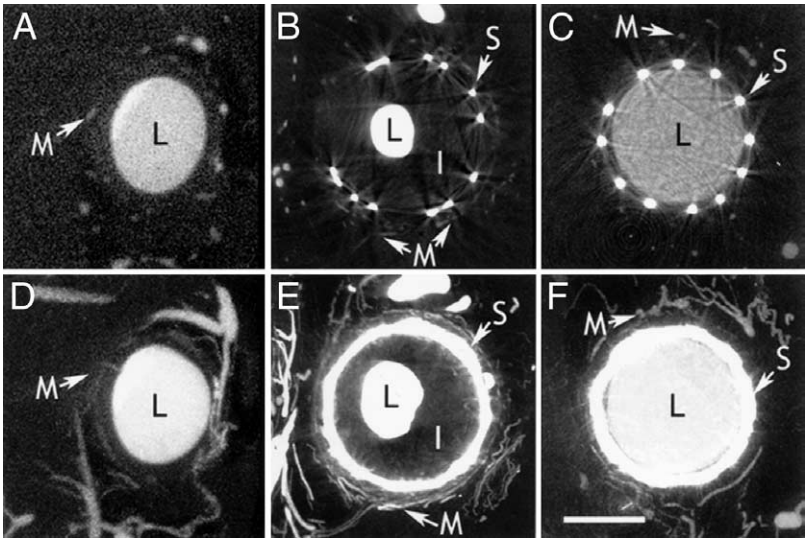

Figure 8. Representative cross-sectional **(A to C)** and maximum intensity projection (MIP) **(D to F)** images obtained from 3D micro CT scans of uninjured **(A, D)**, stented and placebo-treated (**B**, **E**, respectively), and stented and SU11218-treated arteries (**C**, **F**, respectively). The MIP images represent a projection of image intensity along the axial direction, obtained over a 2-mm-thick sample region. **Arrow** = stent. I = intima; L = lumen. Adventitial microvessels (Ad-MV) **(arrowhead)** appear as white dots behind the stent struts in cross-sections and as bright annulus external to the stent in MIP images. There was a significant increase in Ad-MV at 4 weeks after stenting in placebo-treated animals **(B, E)** compared with uninjured arteries **(A, D)** or SU11218-treated animals **(C, F)**. **White bar** = 2 mm.

(34–36). The beneficial effects of VEGF on arterial repair after balloon injury have been attributed to accelerated re-endothelialization (30,35), whereas the untoward effects, stimulation of intimal hyperplasia, might be mediated by recruitment of inflammatory cells (34,37) and promotion of Ad-MV formation (36). The results of VEGF treatment on the development of IH have also been inconclusive in experimental stent injury models. A reduction in the development of IH by VEGF therapy has been reported in some studies (31,33), whereas others have demonstrated a lack of benefit with this approach (32,38).

The conflicting results in both balloon injury and stenting models show the complex relationship between VEGF and the arterial repair process and are likely related to methodological differences among these studies. The effects of angiogenic growth factor or inhibitor administration after arterial injury might be related to the type of injury (balloon vs. stent), extent of injury (superficial vs. deep), site of delivery (intraluminal vs. adventitial), as well as timing and duration of angiogenic growth factor or inhibitor administration. Endothelial denudation with minimal arterial wall damage and/or a brief local/intraluminal VEGF exposure might have a predominant effect of enhanced re-endothelialization of the injured segments, whereas injury to deeper vascular layers and prolonged VEGF exposure, systemic or peri-adventitial, might have an opposite effect on intimal growth by enhancing Ad-MV formation. This latter concept is supported by the inhibition of intimal hyperplasia after balloon injury with inhibitors of angiogenesis (34,36) and now reported in the present study with stent injury. Further studies are required to understand the interactions between various factors contributing to these variable responses.

Conclusions. Arterial stenting is associated with tissue hypoxia in the vessel wall and generates a significant Ad-MV response. A TKI, SU11218, inhibits both the increase in Ad-MV and IH. Compounds like SU11218 might therefore have an important therapeutic role in the prevention of restenosis after arterial stenting.

Acknowledgments

We would like to thank Emile Plise of SUGEN, Inc., for assistance with in vitro SU11218 studies, Cesar Medina and Anand Sistla of SUGEN, Inc., for assistance with compound formulation, and Asaad Nematalla and P. Cho Tang for the supply of SU11218.

Reprint requests and correspondence: Dr. Bradley H. Strauss, Division of Cardiology, St. Michael's Hospital, 30 Bond Street, Toronto, Ontario, Canada M5B 1W8. E-mail: straussb@smh.toronto.on.ca.

REFERENCES

1. Scott NA, Cipolla GD, Ross CE, et al. Identification of a potential role for the adventitia in vascular lesion formation after balloon overstretch injury of porcine coronary arteries. Circulation 1996;93:2178–87.
2. Strauss BH, Robinson R, Batchelor WB, et al. In vivo collagen turnover following experimental balloon angioplasty injury and the role of matrix metalloproteinases. Circ Res 1996;79:541–50.
3. Li C, Cantor WJ, Nili N, et al. Arterial repair after stenting and the effects of GM6001, a matrix metalloproteinase inhibitor. J Am Coll Cardiol 2002;39:1852–8.
4. Kwon HM, Sangiorgi G, Ritman EL, et al. Adventitial vasa vasorum in balloon-injured coronary arteries: visualization and quantitation by a microscopic three-dimensional computed tomography technique. J Am Coll Cardiol 1998;32:2072–9.
5. Pels K, Labinaz M, Hoffert C, O'Brien ER. Adventitial angiogenesis early after coronary angioplasty : correlation with arterial remodeling. Arterioscler Thromb Vasc Biol 1999;19:229–38.
6. Kourembanas S, Hannan RL, Faller DV. Oxygen tension regulates the expression of the platelet-derived growth factor-B chain gene in human endothelial cells. J Clin Invest 1990;86:670–4.
7. Shima DT, Adamis AP, Ferrara N, et al. Hypoxic induction of endothelial cell growth factors in retinal cells: identification and characterization of vascular endothelial growth factor (VEGF) as the mitogen. Mol Med 1995;1:182–93.
8. Abramsson A, Lindblom P, Betsholtz C. Endothelial and nonendothelial sources of PDGF-B regulate pericyte recruitment and influence vascular pattern formation in tumors. J Clin Invest 2003;112:1142–51.
9. Jain RK, Booth MF. What brings pericytes to tumor vessels? J Clin Invest 2003;112:1134–6.
10. Griffin RJ, Williams BW, Wild R, Cherrington JM, Park H, Song CW. Simultaneous inhibition of the receptor kinase activity of vascular endothelial, fibroblast, and platelet-derived growth factors suppresses tumor growth and enhances tumor radiation response. Cancer Res 2002;62:1702–6.
11. Bergers G, Song S, Meyer-Morse N, Bergsland E, Hanahan D. Benefits of targeting both pericytes and endothelial cells in the tumor vasculature with kinase inhibitors. J Clin Invest 2003;111:1287–95.
12. Feldkamp L, Davis L, Kress J. Practical cone-beam algorithm. J Opt Soc Am A 1984;A1:612–9.
13. Schwartz RS, Huber KC, Murphy JG, et al. Restenosis and the proportional neointimal response to coronary artery injury: results in a porcine model. J Am Coll Cardiol 1992;19:267–74.
14. Arteel GE, Thurman RG, Raleigh JA. Reductive metabolism of the hypoxia marker pimonidazole is regulated by oxygen tension independent of the pyridine nucleotide redox state. Eur J Biochem 1998;253:743–50.
15. Raleigh JA, Chou SC, Arteel GE, Horsman MR. Comparisons among pimonidazole binding, oxygen electrode measurements, and radiation response in C3H mouse tumors. Radiat Res 1999;151:580–9.
16. Folkman J. Angiogenesis in cancer, vascular, rheumatoid and other disease. Nat Med 1995;1:27–31.
17. Kaiser M, Younge B, Bjornsson J, Goronzy JJ, Weyand CM. Formation of new vasa vasorum in vasculitis. Production of angiogenic cytokines by multinucleated giant cells. Am J Pathol 1999;155:765–74.
18. Kobayashi M, Matsubara J, Matsushita M, Nishikimi N, Sakurai T, Nimura Y. Expression of angiogenesis and angiogenic factors in human aortic vascular disease. J Surg Res 2002;106:239–45.
19. Kwon HM, Sangiorgi G, Ritman EL, et al. Enhanced coronary vasa vasorum neovascularization in experimental hypercholesterolemia. J Clin Invest 1998;101:1551–6.
20. Shweiki D, Itin A, Soffer D, Keshet E. Vascular endothelial growth factor induced by hypoxia may mediate hypoxia-initiated angiogenesis. Nature 1992;359:843–5.
21. Brogi E, Wu T, Namiki A, Isner JM. Indirect angiogenic cytokines upregulate VEGF and bFGF gene expression in vascular smooth muscle cells, whereas hypoxia upregulates VEGF expression only. Circulation 1994;90:649–52.
22. Namiki A, Brogi E, Kearney M, et al. Hypoxia induces vascular endothelial growth factor in cultured human endothelial cells. J Biol Chem 1995;270:31189–95.
23. Berg JT, Breen EC, Fu Z, Mathieu-Costello O, West JB. Alveolar hypoxia increases gene expression of extracellular matrix proteins and platelet-derived growth factor-B in lung parenchyma. Am J Respir Crit Care Med 1998;158:1920–8.

24. Kourembanas S, Marsden PA, McQuillan LP, Faller DV. Hypoxia induces endothelin gene expression and secretion in cultured human endothelium. J Clin Invest 1991;88:1054–7.
25. Muraoka K, Shimizu K, Sun X, et al. Hypoxia, but not reoxygenation, induces interleukin 6 gene expression through NF-kappa B activation. Transplantation 1997;63:466–70.
26. Kietzmann T, Roth U, Jungermann K. Induction of the plasminogen activator inhibitor-1 gene expression by mild hypoxia via a hypoxia response element binding the hypoxia-inducible factor-1 in rat hepatocytes. Blood 1999;94:4177–85.
27. Bjornheden T, Bondjers G. Oxygen consumption in aortic tissue from rabbits with diet-induced atherosclerosis. Arterioscler Thromb 1987;7:238–47.
28. Moulton KS, Heller E, Konerding MA, Flynn E, Palinski W, Folkman J. Angiogenesis inhibitors endostatin or TNP-470 reduce intimal neovascularization and plaque growth in apolipoprotein E-deficient mice. Circulation 1999;99:1726–32.
29. Moulton KS, Vakili K, Zurakowski D, et al. Inhibition of plaque neovascularization reduces macrophage accumulation and progression of advanced atherosclerosis. Proc Natl Acad Sci U S A 2003;100: 4736–41.
30. Asahara T, Bauters C, Pastore C, et al. Local delivery of vascular endothelial growth factor accelerates reendothelialization and attenuates intimal hyperplasia in balloon-injured rat carotid artery. Circulation 1995;91:2793–801.
31. Van Belle E, Tio FO, Chen D, Maillard L, Kearney M, Isner JM. Passivation of metallic stents after arterial gene transfer of phVEGF165 inhibits thrombus formation and intimal thickening. J Am Coll Cardiol 1997;29:1371–9.
32. Swanson N, Hogrefe K, Javed Q, Malik N, Gershlick AH. Vascular endothelial growth factor (VEGF)-eluting stents: in vivo effects on thrombosis, endothelialization and intimal hyperplasia. J Invasive Cardiol 2003;15:688–92.
33. Walter DH, Cejna M, Diaz-Sandoval L, et al. Local gene transfer of phVEGF-2 plasmid by gene-eluting stents: an alternative strategy for inhibition of restenosis. Circulation 2004;110:36–45.
34. Ohtani K, Egashira K, Hiasa K, et al. Blockade of vascular endothelial growth factor suppresses experimental restenosis after intraluminal injury by inhibiting recruitment of monocyte lineage cells. Circulation 2004;110:2444–52.
35. Hutter R, Carrick FE, Valdiviezo C, et al. Vascular endothelial growth factor regulates reendothelialization and neointima formation in a mouse model of arterial injury. Circulation 2004;110: 2430–5.
36. Khurana R, Zhuang Z, Bhardwaj S, et al. Angiogenesis-dependent and independent phases of intimal hyperplasia. Circulation 2004;110: 2436–43.
37. Zhao Q, Egashira K, Hiasa K, et al. Essential role of vascular endothelial growth factor and Flt-1 signals in neointimal formation after periadventitial injury. Arterioscler Thromb Vasc Biol 2004;24: 2284–9.
38. Hedman M, Hartikainen J, Syvanne M, et al. Safety and feasibility of catheter-based local intracoronary vascular endothelial growth factor gene transfer in the prevention of postangioplasty and in-stent restenosis and in the treatment of chronic myocardial ischemia: phase II results of the Kuopio Angiogenesis Trial (KAT). Circulation 2003; 107:2677–83.